Available online at www.sciencedirect.com

ScienceDirect

Energy Procedia 110 (2017) 121 – 127

Energy Procedia

1st International Conference on Energy and Power, ICEP2016, 14-16 December 2016, RMIT University, Melbourne, Australia

Electrochemical synthesis of core-shell ZnO/CdS nanostructure for photocatalytic water splitting application

Avinash Rokade[a], Sachin Rondiya[a], Abhijit Date[b], Vidhika Sharma[c], Mohit Prasad[c], Habib Pathan[c], Sandesh Jadkar[c,*]

[a]*School of Energy Studies,Savitribai Phule Pune University,Pune and 411007, India*
[b]*School of Engineering, RMIT University, Melbourne 3000, Australia*
[c]*Department of Physics,Savitribai Phule Pune University, Pune, 411007, India*

Abstract

We have successfully synthesized ZnO NRs and ZnO/CdS core-shell structures by a facile two step chemical routes viz. electrodeposition and chemical bath deposition. Plane ZnO nanorods films were deposited by using three electrode electrodeposition on FTO glass substrates. The ZnO/CdS core-shell structures were deposited by immersing plane ZnO nanorod films into a bath containing precursor solution of CdS in chemical bath deposition. Formation of ZnO NRs and ZnO/CdS core-shell structures has been confirmed by UV-Visible absorption, Raman spectroscopy and scanning electron microscopy. The synthesized ZnO NRs and ZnO/CdS core-shell structures has been also characterized for photoelectrochemical (PEC) properties, Mott-Schottky analysis, electrochemical impedance spectroscopy (EIS) and efficiency measurements of PEC system. It has been found that the photocurrent conversion efficiency in water splitting is higher for ZnO/CdS core-shell photoanode than ZnO NRs photoanode. These results suggest that addition of CdS with ZnO NRs is beneficial in increasing the visible light absorption and to enhance the photocurrent conversion efficiency in water splitting. Thus, ZnO/CdS core-shell configuration can be a prospective candidate for efficient PEC splitting of water.

Peer-review under responsibility of the organizing committee of the 1st International Conference on Energy and Power.

* Corresponding author. Tel.: +91 20 2569 5201; fax: +91 20 2569 5201.
E-mail address: sandesh@physics.unipune.ac.in

Peer-review under responsibility of the organizing committee of the 1st International Conference on Energy and Power.
doi:10.1016/j.egypro.2017.03.116

*Keywords:*Electrochemical deposition; Core-shell ZnO; Water Splting; Scanning electron microscopy.

1. Introduction

Zinc oxide (ZnO) is a group II-VI compound semiconductor material with a direct wide band gap of ~ 3.37 eV and a large exciton binding energy of ~ 60 meV at room temperature [1]. It is a promising material with broad applications in optoelectronics, transistors, UV sensors, biosensors, gas sensors, photo-catalyst etc. due to its excellent opto-electronic properties. One-dimensional (1D) nanostructures of ZnO such as nanoparticles [2, 3], nanotubes [4], nanoflowers [5], nanowires [6], tetrapods [7], nanorods [8], doughnuts [9], nanodisks, nanoplates, nanospheres and hemispheres [10-15] nanosheets [16], etc. are ideal photo-catalysts because of their large surface-to-volume ratio. To sensitize ZnO, cadmium sulphide (CdS) is an excellent material due to its advantages for visible light harvesting, high abundance and low-cost production. Especially it has an appropriate band alignment with ZnO [17, 18]. The band alignment of ZnO with CdS results highly efficient separation of photo-generated charge carriers. However, ZnO/CdS have rarely been explored for the visible-light driven applications.[19,20] The core shell nano-composites have a lot of advantages over planar thin films semiconductor junction such as large surface area for photons to interact with material and to reduce electron hole recombination losses.

The ZnO has higher carrier mobility and hence addition of CdS layer with ZnO as a visible active layer enhances the light absorption process. The synthesized hierarchical morphologies ZnO/CdS core-shell structure shows a prominent visible-light-driven performance under the light irradiation. The ability to form 1D nanostructures of ZnO with uniform CdS shell layers is a key step toward the realization of high-efficiency photoelectrochemical (PEC) cells.[20,21] Here, we report synthesis of ZnO nanorods (ZnO NRs) and ZnO/CdS core-shell by a facile two step chemical routes. The morphology, optical properties, and PEC performance of ZnO NRs and ZnO/CdS core-shell have been investigated in view of their use in water slitting.

2. Experimental

2.1. Synthesis of ZnO NRs and ZnO/CdS core-shell

ZnO nanorods were synthesized on FTO glass substrate by simple, cost effective and environment friendly electrodeposition method. The FTO substrate, Pt foil and SCE were used as working, counter and reference electrodes respectively. The required electrodeposition parameters are such as deposition potential, time, temperature and molarities were optimized for well aligned, dense and uniform growth of ZnO nanorods. The aqueous solution of equimolar zinc nitrate [$Zn(NO_3)_2.6H_2O$] and hexamethylenetetramine (HMT) (both AR grade, 99.99% pure) precursors were kept at temperature ~ 80 ^{0}C throughout experiment. A constant potential ~ - 0.75 V was applied for 4 hours to grow sufficiently high dense nanorods on the substrate surface.

The CdS thin films were deposited independently on FTO glass substrate by using CBD method. For synthesis of CdS films specific molarities of cadmium sulphate ($CdSO_4$), thiourea and ammonium hydroxide were kept constant to maintain pH of solution at 11. Then ZnO NRs films were dipped inside a solution at temperature 70 ^{0}C and finally CdS shell layer was grown with optimum thickness on ZnO nanorod films. The synthesized films were removed and dried under air flux.

2.2. Characterization of ZnO NRs and ZnO/CdS core-shell

The surface morphology of the films was investigated using a JEOL JSM-6360A scanning electron microscope (SEM) with operating voltage 20 kV. The optical band gap of the films was deduced from absorption and was measured using a JASCO, V-670 UV-Visible spectrophotometer in the range of 200-800 nm. Raman spectra were recorded with Raman spectroscopy (Jobin Yvon Horibra LABRAM-HR) in the range 150-900 cm^{-1}. The excitation source was 632.8 nm line of He-Ne laser. The power of the Raman laser was kept less than 5 mW to avoid laser induced crystallization on the films.

2.3. Photoelectrochemical (PEC) cell assembly

The grown ZnO NRs and ZnO/CdS core-shell photoanodes were used as working electrode (WE) in PEC cell. Three electrodes were placed inside the cell; ZnO NRs and ZnO/CdS core-shell photoanodes as working electrode (WE), platinum foil counter electrode (CE), and saturated calomel reference electrode (SCE). 0.5 M Na_2SO_4 was used as an electrolyte. Potentiostat (Metrohm Autolab PGSTAT302N) and 150 W Xenon Arc Lamp (PEC-L01) with illumination intensity of 100 mW/cm^2 (AM 1.5) were employed to record current-voltage (I-V) characteristics. Electrochemical impedance spectroscopy (EIS) measurements were carried out using same potentiostat (Model: FRA 32M). The PEIS measurements were recorded in 0.5 M Na_2SO_4 electrolyte at 0.5 V and the frequency was kept in the range of 0.1 Hz to 100 KHz. The Mott-Schottky (MS) plot of Z-NRs samples ($1/C^2$ vs. electrode potential) were recorded under darkness at a frequency of 500 Hz to obtain flat band potential (V_{fb}), donor density (N_d) and width of space charge layer (w) [22, 23]. AR grade reagents and double distilled water (specific conductance < 10^{-6} mho cm^{-1}) was used throughout the experiment.

3. Results and Discussion

3.1. Raman spectroscopy analysis

Formation of ZnO NRs and ZnO/CdS core-shell has been confirmed by Raman spectroscopy and is shown in Fig. 1.

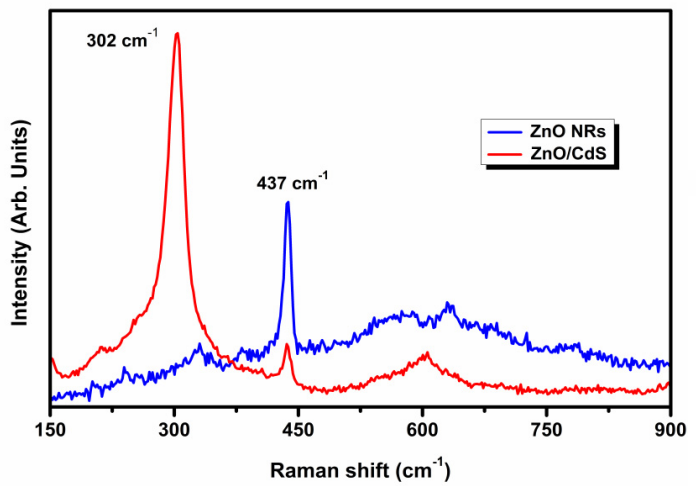

Fig. 1. Raman spectra of ZnO and ZnO/CdS core-shell

The strongest evidence of Wurtzite ZnO structure formation comes from Raman spectroscopy analysis. Fig. 1 shows a strong Raman peak centered ~ 437 cm^{-1}, which corresponds to the E_2 high frequency mode of ZnO involving mainly Zn motion corresponding to the band characteristic of the Wurtzite phase [24-26]. The presence of hexagonal Wurtzite CdS is also confirmed by observing two Raman shoulders one centered ~ 302 cm^{-1} and other weak peak centered ~ 600 cm^{-1} cm^{-1} [19, 27]. For ZnO/CdS core-shell Raman spectra show three distant peaks, ~ 302 cm^{-1} and ~ 600 cm^{-1}, and ~ 437 cm^{-1}, corresponding to longitudinal optic (LO) vibrational nodes of ZnO and CdS confirming the formation of core-shell of ZnO/CdS. For ZnO/CdS core-shell sample CdS has suppressed Raman scattering compared to ZnO which may be due to absorption of photons by the CdS coatings.

3.2. Scanning electron microscopy (SEM) analysis

Figure 2 shows SEM micrographs of ZnO thin films and ZnO/CdS core-shell. The SEM micrographs for both films

show nice surface morphology with uniform, dense and highly crystalline hexagonal nanorods formation. Table 1 gives summary of nanorod density, average diameter and growth length of ZnO nanorods and ZnO/CdS core-shell nanostructures. As seen from the table the density, average diameter and average length of ZnO NR and ZnO/CdS core-shell were found ~ 400x10^{-2} µm^{-2}, 140 nm, 1600 nm and 300x10^{-2} µm^{-2}, 250 nm, 1700 nm respectively.

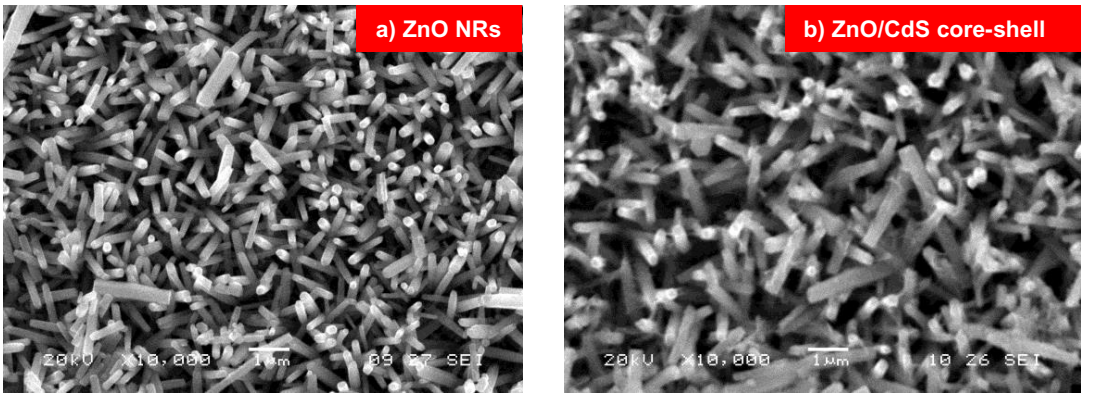

Fig. 2. Scanning electron microscopy images of a**)** ZnO NRs and **b)** ZnO/CdS core-shell structure.

Table 1. Growth density, average diameter and growth length of ZnO NRs and ZnO/CdS coreshell nanostructures.

Estimated parameters of ZnO nanorods	**ZnO NRs**	**ZnO/CdS Core-shell**
Nanorod density (10^{-2} µm^{-2})	400	300
Average diameter of nanorods (nm)	140	250
Average Length of nanorods (nm)	~ 1600	~ 1700

3.3. UV-Visible spectroscopy analysis

Fig. 3 shows the UV-Visible optical absorption spectra of ZnO and ZnO/CdS core-shell nanostructures used to calculate band gap of films. The extrapolations of the curves to the energy axis at zero absorption gives absorption edges which approximately corresponds to the band gap energies of ZnO and ZnO/CdS core-shell nanostructures.

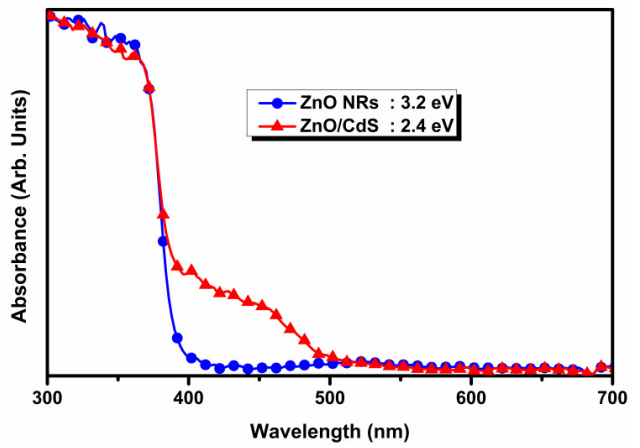

Fig. 3. UV-Visible absorption spectra of ZnO and ZnO/CdS core-shell nanostructure. Estimated band gap values are also shown in the figure.

The estimated band gap values are 3.2 eV and 2.4 eV for ZnO and ZnO/CdS core-shell respectively. These measurements indicate the presence of both phases in the film, CdS and ZnO. These values of band gap are consistent with values reported in literature [28-30].

3.4. Photoelectrochemical activity analysis

The Photoelectrochemical activity of ZnO NRs and ZnO/CdS core-shell photoelectrode was evaluated using linear sweep voltammetry (LSV) technique. The measurements were conducted with three-electrode cell at – 1.0 to 1.0 V vs. SCE in 0.5 M Na_2SO_4 electrolyte. The plots of photocurrent (I) versus applied bias (V) are presented in Fig. 4(a). A very small current of ~ 0.01 μA/cm^2 was observed during measurement of current in dark because of non-faradic reaction. Upon illumination, direct photoexcitation of ZnO would occur, leading to the generation of electron-hole pairs. The photo-generated electrons would be driven to the Pt counter electrode (cathode) to generate H_2 through the reduction of protons, while the photo-generated holes would react with water to generate O_2. Thus the photocurrent density for ZnO/CdS core-shell photoanodes is higher than ZnO NRs photoanodes. It is interesting to note that the prepared ZnO NRs and ZnO/CdS core-shell photoelectrodes were found to be stable even after multiple scans and there was no physicochemical degradation observed which the stability of configured systems for water splitting reaction.

In order to estimate the lifetime of photocarriers electrochemical impedance spectroscopy (EIS) was performed under illumination as shown in Fig. 4(b). Normally, smaller arc radius on the EIS Nyquist plot indicates an effective separation of photo-generated electron-hole pairs and a fast interfacial charge transfer process. The smaller diameter of ZnO/CdS core-shell photoanodes implies a likely prolonged lifetime of photo generated carriers compared with ZnO NRs photoanodes.

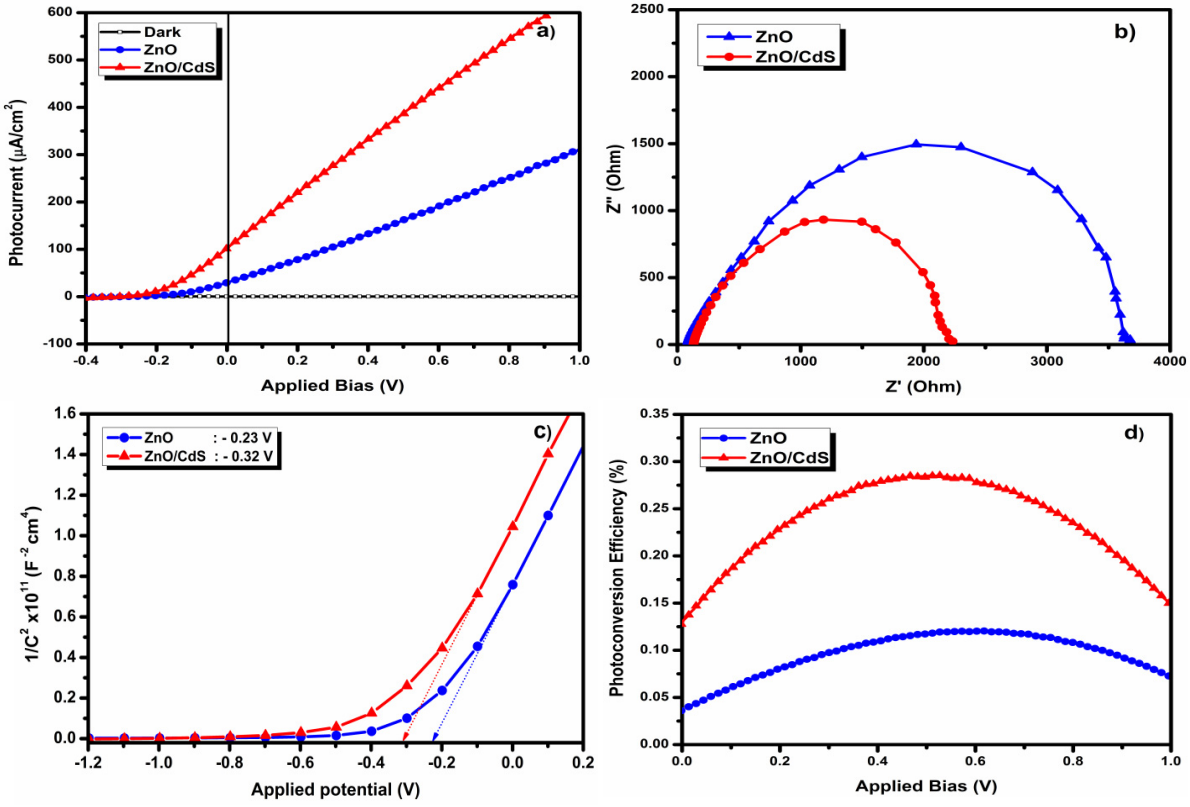

Fig. 4. Electrochemical activity of ZnO NRs and ZnO/CdS core-shell **a)** Change in photocurrent density as a function of applied bias potential **b**) Nyquist plots **c)** Mott-Schottky plots and **d)** photo conversion efficiency of PEC cell

Capacitance was derived from the electrochemical impedance at each potential with 500 Hz frequency in dark is shown in Fig 4(c) (Mott-Schottky). As seen both ZnO NRs and ZnO/CdS core-shell samples exhibited positive slopes, indicating both ZnO NRs and ZnO/CdS core-shell photoelectrodes retain n-type behavior. Compared to ZnO NRs, ZnO/CdS core-shell photoelectrodes indicates much higher charge carrier density. The flat band potential, charge carrier density and the width of the space-charge layer are calculated, and summarized in Table 2.

Table 2. Comparative efficiency parameters obtained for ZnO & ZnO/CdS core shell photo electrode

Sample	Charge carrier density N_d (cm^{-3})	Flat band potential V_{fb} (Volt)	Width of space-charge layer w (nm)
ZnO NR	$5x10^{17}$	-0.23	16
ZnO/CdS core shell	$2x10^{18}$	-0.32	28

The PCE of all the fabricated samples was calculated using,

$$PEC = \frac{J_{Ph}\ (1.23 - |V_{Bias}|}{P_{Light}} \quad (1)$$

Where J_{ph} is the photocurrent density (mA cm^{-2}), P_{light} is the incident light intensity (100 mW cm^{-2}), and V_b is the applied bias potential. Here, V_{Bias} is the difference between the potential at the measuring point and the electrode open-circuit potential under the same illumination intensity. As shown in Fig. 4(d), for ZnO NRs photoanodes maximum PCE is 0.12 % and for ZnO/CdS core-shell photoanodes it is 0.29 % at 0.5 V. All the results suggest that addition of CdS with ZnO NRs is beneficial in increasing the light absorption and leads to an improvement of the photocurrent conversion efficiency in water splitting. Thus, ZnO/CdS core-shell configuration can be a prospective candidate for efficient PEC splitting of water.

4. Conclusions

We have successfully synthesized ZnO NRs and ZnO/CdS core-shell structures by a facile two step chemical routes viz. electrodeposition and chemical bath deposition. Formation of ZnO NRs and ZnO/CdS core-shell structures has been confirmed by UV-Visible absorption, Raman spectroscopy and scanning electron microscopy. The obtained films are also characterized for photoelectrochemical (PEC) properties, Mott-Schottky analysis, electrochemical impedance spectroscopy (EIS) and efficiency measurements of PEC system. It has been observed that the photocurrent conversion efficiency in water splitting is higher for ZnO/CdS core-shell photoanode than ZnO NRs photoanode. These results suggest that addition of CdS with ZnO NRs is beneficial in increasing the light absorption and to enhance the photocurrent conversion efficiency in water splitting. Thus, ZnO/CdS core-shell configuration can be a prospective candidate for efficient PEC splitting of water.

Acknowledgement

Avinash Rokade is grateful to Ministry of New and Renewable Energy (MNRE), New Delhi for National Renewable Energy (NRE) fellowship and financial assistance. Sachin Rondiya gratefully acknowledges the financial support from Dr. Babasaheb Ambedkar Research and Training Institute (BARTI), Pune, for the award of Junior Research Fellowship. Vidhika Sharma and Mohit Prasad are thankful to University Grants Commission, Government of India, New Delhi for Dr. D. S. Kothari Postdoc Fellowship. Sandesh Jadkar is thankful to University Grants Commission, New Delhi for special financial support under UPE program.

References

[1] Ozgur U, Alivov YI, Liu C, Teke A, Reshchikov MA, Dogan S, Avrutin V, Cho SJ, Morkoc H. A comprehensive review of ZnO materials and devices. J. Appl. Phys. 2005;98:041301-1-103.

[2] Kawano T, Imai H. Fabrication of ZnO Nanoparticles with Various Aspect Ratios through Acidic and Basic Routes. Cryst Growth Des 2006;6:1054-1056.
[3] Masuda Y, Kato K. Self-Standing Particle-Binding ZnO Films. J Nanosci Nanotech 2009; 9:433-438.
[4] Xing YJ, Xi ZH, Zhang XD, Song JH, Wang RM, Xu J, Xue ZQ, Yu DP. Nanotubular structures of Zinc Oxide. Solid State Commun 2004; 129:671-675.
[5] Liu JP, Huang XT, Li YY, Sulieman KM, Sun FL, He X. Selective growth and properties of zinc oxide nanostructures. Scr Mater 2006;55: 795-798.
[6] Su Y, Li L, Chen Y, Zhou Q, Gao M, Chen Q, Feng Y. The synthesis of Sn-doped ZnO nanowires on ITO substrate and their optical properties. J Cryst Growth 2009;311:2466-2469.
[7] Chen ZG, Ni A, Li F, Cong HT, Cheng HM, Lu GQ. Synthesis and photoluminescence of tetrapod ZnO nanostructures. Chem Phys Lett 2007;434:301-305.
[8] Zhao J,Jin ZG, Li T, Liu XX. Preparation and characterisation of ZnO nanorods from NaOH solutions with assisted electrical field. Appl Surf Sci 2006;252:8287-8294.
[9] Ghoshal T, Kar S, Chaudhuri S. ZnO Doughnuts: Controlled Synthesis, Growth Mechanism, and Optical properties. Cryst Growth Des 2007;7:136-141.
[10] Bardhan R, Wang H, Tam F, Halas NJ. Facile Chemical Approach to ZnO Submicrometer Particles with Controllable Morphologies. Langmuir 2007; 23:5843-5847.
[11] Xu F, Yuan ZY, Du GH, Halasa M, Su BL. High-yield synthesis of single crystalline ZnO hexagonal nanoplates and accounts of their optical and photocatalytic properties. Appl Phys A 2007;86:181-185.
[12] Jang ES, Won JH, Hwang SJ, Choy JH. Fine Tuning of the Face Orientation of ZnO Crystals to Optimize Their Photocatalytic Activity. Adv Mater 2006;18:3309-3312.
[13] Illy B, Shollock BA, Driscoll JL, Ryan MP. Electrochemical growth of ZnO nanoplates. Nanotechnology 2005;16:320-324.
[14] Gao P, Ying C, Wang SQ, Ye LN, Guo QX, Xie Y. Low temperature hydrothermal synthesis of ZnO nanodisk arrays utilizing self- assembly of surfactant molecules at solid-liquid interface. J Nanopart Res 2006;8:131-136.
[15] Niu HX, Yang Q, Tang KB, Xie Y, Yu F. Self-assembly of ZnO nanoplates into microspheres. Mater Sci 2006;41:5784-5787.
[16] Pradhan D, Leung KT. Vertical Growth of Two-Dimensional Zinc Oxide Nanostructures on ITO-Coated Glass:Effects of Deposition Temperature and Deposition Time. J Phys Chem C 2008;112:1357-1364.
[17] Olson DC, Lee Y, White MS, Kopidakis N, Shaheen SE, Voigt JA, Hsu JWP. Effect of Polymer Processing on the Performance of Poly(3-hexylthiophene)/ZnO Nanorod Photovoltaic Devices J Phys Chem C 2007;111:16640-45.
[18] Bao N, Shen L, Takata T, Domen K, Gupta A, Yanagisawa K, Grimes CA. Facile Cd-Thiourea Complex Thermolysis Synthesis of Phase-Controlled CdS Nanocrystals for Photocatalytic Hydrogen Production under Visible Light. J Phys Chem C 2007;111:17527-17534.
[19] Nayak J, Sahu SN, Kasuya J, Nozaki S. CdS-ZnO composite nanorods: Synthesis, characterization and application for photocatalytic degradation 3,4-dihydroxy benzoic acid. Applied Surface Science 2008;254:7215-7218.
[20] Khanchandani S, Kundu S, Patra A, Ganguli AK. Shell Thickness Dependant Photocatalytic Properties of ZnO/CdS Core-Shell nanorods. J Phys Chem C 2012;116:23653-23662.
[21] Yang X, Yang Q, Hu Z, Guo S, Li Y, Sun J, Xu N, Wu J. Extended photoresponce of ZnO/CdS core/shell nanorods to solar radition and related mechanisms. Solar Energy Materials and Solar Cells 2015;137:169-174.
[22] Mora-Sero I, Fabregat-Santiago F, Denier B, Bisquert J, Tena-Zaera R, Elias J, Levy-Clement C. Determination of carrier density of ZnO nanowires by electrochemical techniques. Appl Phy Lett 2006;89:203117-1-3.
[23] Fabregat-Santiago F, Garcia-Belmonte G, Bisquert J, Bogdanoff P, Zaban A. Mott-Schottky analysis of nanoporous semiconductor electrodes in dielectric state deposited on SnO_2(F) conducting substrates. Journal of The Electrochemical Society 2003;150:E293-E298.
[24] Li C, Lva Y, Guo L, Xu H, Ai X, Zhang J. Raman and exitonic photoluminescence characterizations of ZnO sta-shaped nanocrystals. Journal of Luminescence 2007;122:415-417.
[25] Moura AP, Lima RC, Moreira ML. ZnO architectures synthesized by a microwave-assisted hydrothermal method and their photoluminescence properties. Solid State Ionics 2010;181/15:775-780.
[26] Li C, Zhang J, Yu H, Zhang L. Raman and Photoluminescence Properties of ZnO Nanorods with Wurtzite Structure. Engineering Materials. 2013;538:50-53.
[27] Hu C, Zeng X, Cui J, Chen H, Lu J. Size Effects of Raman and Photoluminescence Spectra of CdS Nanobelts. J Phys Chem C 2013;117:20998−21005.
[28] Kathalingam A, Kim MR, Chae YS, Rhee JK, Mahalingam T. Studies on Electrochemically Deposited ZnO Thin Films. J Korean phys Soc 2009;55/6:2476-2481.
[29] Fan D, Thomas PJ, O'Brien P. Deposition of CdS and ZnS thin films at the water /touene interface. J Mater Chem 2007;17:1381-1386.
[30] Ouachtari F, Rmili A, Elidrissi SEB, Bouaoud A, Erguig H, Elies P. Influence of Bath Temperature, Deposition Time and [S]/[Cd] Ratio on the Structure, Surface Morphology, Chemical Composition and Optical Properties of CdS Thin Films Elaborated by Chemical Bath Deposition. J of Modern Phys 2011;2:1073-1082.